ORIGINAL RESEARCH PAPER

Review of strength models for masonry spandrels

Katrin Beyer · Sujith Mangalathu

Abstract   Many older unreinforced masonry (URM) buildings feature timber floors and solid brick masonry. Simple equivalent frame models can help predicting the expected failure mechanism and estimating the strength of a URM wall. When modelling a URM wall with an equivalent frame model rather than, for example, a more detailed simplified micro-model, the strengths of the piers and spandrels need to be estimated from mechanical or empirical models. Such models are readily available for URM piers, which have been tested in many different configurations. On the contrary, only few models for spandrel strength have been developed. This paper reviews these models, discusses their merits, faults and compares the predicted strength values to the results of recent experimental tests on masonry spandrels. Based on this assessment, the paper outlines recommendations for a new set of strength equations for masonry spandrels.

Keywords   Masonry spandrels · Strength models · Peak strength · Residual strength · Brick masonry · Unreinforced masonry

1 Introduction

Most performance-based seismic assessment methods require the computation of a push-over curve. A number of analysis tools, with different degrees of sophistication, have been developed for unreinforced masonry (URM) buildings, which constitute a large part of the

K. Beyer (✉) · S. Mangalathu
Ecole Polytechnique Fédérale de Lausanne (EPFL), Lausanne, Switzerland
e-mail: katrin.beyer@epfl.ch

K. Beyer
School of Architecture, Civil and Environmental Engineering, EPFL ENAC IIC EESD,
GC B2 504, Station 18, 1015 Lausanne, Switzerland

S. Mangalathu
IUSS-Rose school, 27100 Pavia, Italy

worldwide building stock. Reviews of such tools can be found, for example, in Magenes and Menon (2009) and Penna (2010). While the level of sophistication of any one method is reflected in its computational costs and the expertise required to apply the method, it also often determines the manner in which the spandrel elements are treated. Simple methods typically consider a limit case in which the spandrels are either neglected or considered to be infinitely rigid and strong (e.g., the storey mechanism model by Tomaževič 1987). Such simple methods are suitable for an initial assessment of a building or when the geometry of the wall justifies the limit assumptions on the spandrels as a reasonable approximation of the expected behaviour. However, in most URM buildings, piers and spandrels both contribute to the overall flexibility and it will be difficult to predict the mechanism that will form when the building is subjected to seismic loading. For this reason, URM buildings are often analysed using more advanced models that account for the flexibility and limited strength and deformation capacity of piers and spandrels. Finite element modelling approaches for the nonlinear analysis of URM buildings can be classified as micro models (e.g., Lourenço 1996), macro models (e.g., Gambarotta and Lagomarsino 1997) and equivalent frame models. Of the three approaches, the equivalent frame models are often chosen for the analysis of entire buildings as they are the least expensive computationally. Equivalent frame models have been developed by a number of research groups. Among the first were Braga and Liberatore (1990) and Magenes and Della Fontana (1998). Today, the equivalent frame analysis programs "Tremuri" (Lagomarsino et al. 2006) and "SAM" (Magenes et al. 2006) have been developed to a level that makes the nonlinear analysis of URM buildings feasible in engineering practice.

Most equivalent frame models require strength formulations for URM piers and spandrels that are closed-form expressions, and therefore equations derived from simple mechanical strength models are often best suited for the implementation in equivalent frame models. For URM piers, several such strength models have been proposed by different authors (e.g., Turnšek and Čačovič 1970; Magenes and Calvi 1997). For URM spandrels, such strength models are rather scarce because experimental data on URM spandrels, which is required for the validation of the models, was not available until recently. Nevertheless, a number of scientific papers and design codes have proposed models for estimating the strength of masonry spandrels. The objective of this paper is to summarise the existing strength models, to review them in the light of new experimental tests on masonry spandrels and to outline recommendations for a revised set of strength equations for masonry spandrels. As an introduction to the topic, the paper commences with the review of experimental results for masonry spandrels and some observations on the force-deformation behaviour of masonry spandrels gained from quasi-static cyclic tests.

The paper addresses only solid brick URM spandrels in existing URM buildings with timber floors (Fig. 1), which are simply referred to as masonry spandrels. Neither stone masonry spandrels (e.g., Calderoni et al. 2008; Graziotti et al. 2009), reinforced masonry spandrels (Haach et al. 2012) nor composite masonry spandrels consisting of a RC beam and a masonry spandrel (Beyer and Dazio 2012b) are considered in this paper. These types of spandrels are excluded as experimental tests have revealed that such spandrel elements exhibit behaviour that is different from that of masonry spandrels.

2 Experimental tests on masonry spandrel elements

The first experimental observations of the behaviour of masonry spandrels in URM buildings subjected to seismic loading stem from shake table tests or quasi-static cyclic tests on URM building models. Benedetti et al. (1998, 2001), for example, tested 24 two-storey URM

Fig. 1 Old URM building during the L'Aquila earthquake on April 6th, 2009, showing spandrel failure **a** and detail of a spandrel test unit (**b**, Beyer and Dazio 2012a)

buildings at half-scale and observed that damage to the spandrels is the mechanism that, for the types of buildings tested, has the largest energy absorption capacity. Quasi-static cyclic tests on URM buildings (e.g., Magenes et al. 1995; Yi et al. 2006) and subassemblages (e.g., Foraboschi 2009; Augenti et al. 2011) revealed further insights into the interaction of piers and spandrels. However, because buildings and subassemblages are statically indeterminate systems, the internal forces of the spandrels are not known exactly but can only be estimated based on assumed stiffness and strength values for the spandrels and piers. Tests of subassemblages are valuable for the validation of models comprising piers and spandrels; for the development of models for the spandrel element, test setups with which the internal forces of the spandrel element can be measured are better suited. Such test setups were recently developed by Gattesco et al. (2008), Graziotti et al. (2009) and Beyer and Dazio (2012a); a comparison of the different test setups is included in the latter.

Gattesco et al. (2008) and Beyer and Dazio (2012a) tested brick masonry spandrels. Gattesco et al. (2008) tested two different masonry spandrels—one with a timber lintel and one with a timber lintel parallel to a flat arch. Beyer and Dazio (2012a) tested four masonry spandrels that featured either a timber lintel or a shallow masonry arch. These tests on masonry spandrels are briefly introduced in the following section, and the results are used to highlight typical features of the force-deformation behaviour of masonry spandrels.

2.1 Test units and test setup

Quasi-static cyclic testing was carried out on four test units, which represented masonry spandrel elements and the adjacent piers (Table 1). Out of the four test units, two featured masonry spandrels with timber lintels and two included masonry spandrels with shallow masonry arches (Fig. 2). Figure 3 shows the test setup. It imposed a drift on the two piers, which defined the deformation demand on the spandrel. Horizontal tie rods restrained the axial elongation of the spandrels. For two test units (TUA and TUC), the axial force in the spandrel was kept constant throughout the test while for the other two test units (TUB and TUD), the axial force in the spandrel depended on the axial elongation of the spandrel and the stiffness and strength of the tie rods.

Table 1 Material properties and details of the application of the axial load for the four spandrel elements (Beyer and Dazio 2012a)

Test unit	Spandrel type	σ_{pier} (MPa)	c (MPa)	$\mu (-)$	f_{cm} (MPa)	f_{tb} (MPa)	Axial force in the spandrel (P_{sp})
TUA	Timber lintel	0.33	0.35	0.85	14.4	8.5	Constant first 80 kN, then 40 kN
TUB	Timber lintel	0.33	0.35	0.85	14.4	7.0	Variable, plain bars with low axial stiffness
TUC	Masonry arch	0.43	0.18	0.73	16.5	6.5	Constant 80 kN
TUD	Masonry arch	0.43	0.18	0.73	16.5	5.0	Variable, plain bars with high axial stiffness

σ_{pier} Mean vertical stress on piers, c cohesion of mortar joint, μ coefficient of friction of mortar joint, f_{cm} compressive strength of masonry, f_{tb} tensile strength of brick
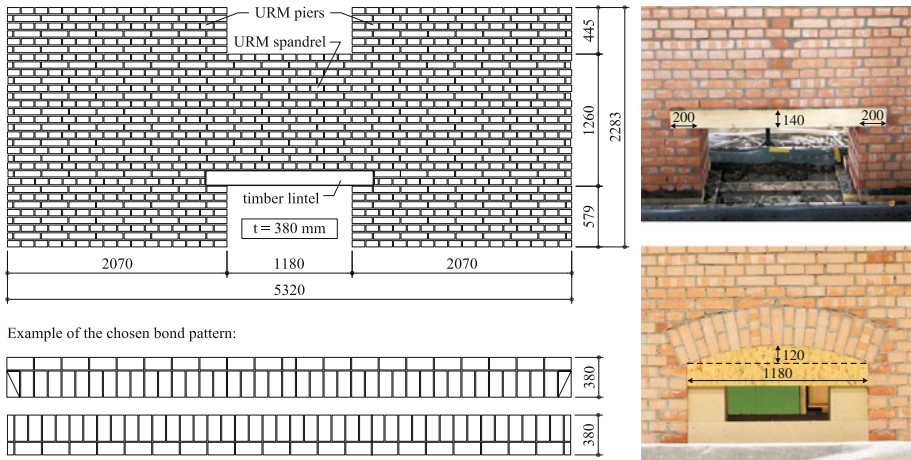

Fig. 2 Geometry of the four spandrel elements tested under quasi-static cyclic loading (Beyer and Dazio 2012a)

In addition to the quasi-static cyclic tests, material tests were carried out to determine the mechanical properties of the construction materials. Those material properties, which are required for the prediction of the spandrel strength (Sect. 5), are summarised in Table 1. Note that TUA and TUB, as well as TUC and TUD, were constructed pairwise at the same time. For each construction phase, only one set of compression tests and shear triplets was constructed and tested; for this reason, the masonry strengths of TUA/TUB and TUC/TUD are assumed to be equal.

2.1.1 Selected experimental results

The results of recent quasi-static cyclic tests have shown that the force-deformation behaviour of masonry spandrels often has the following characteristics (Fig. 4a): up to the peak strength, the shear force in the spandrel increases almost linearly, and the cracks in the spandrel remain
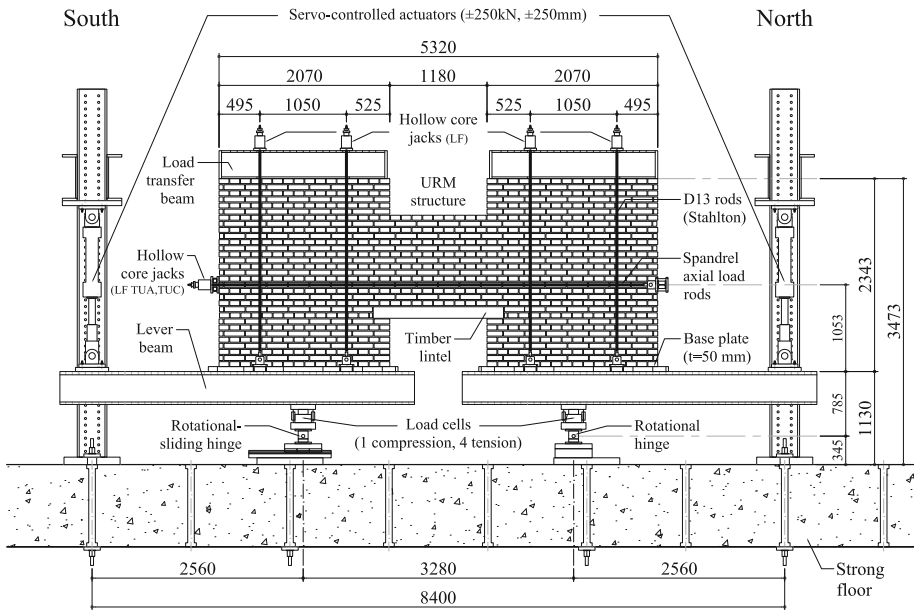
Fig. 3 Test setup for spandrel tests. The side restraint is not shown. All dimensions are in (mm). LF = hollow core jacks connected to load follower, which maintains constant oil pressure (Beyer and Dazio 2012a)
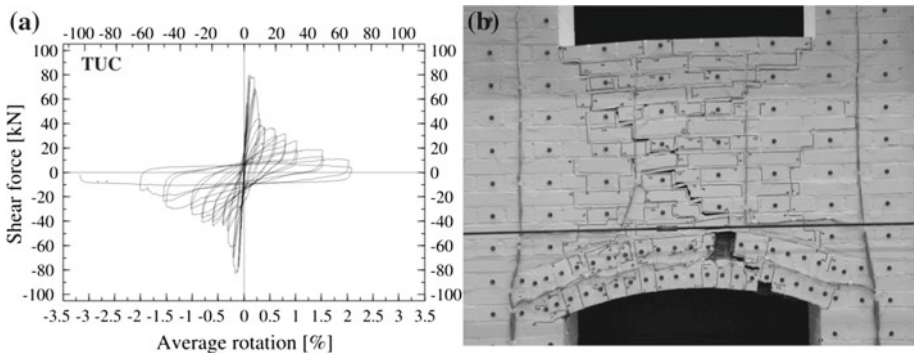
Fig. 4 Shear force-rotation relationship **a** and shear failure mechanism **b** (test unit TUC in Beyer and Dazio 2012a)

rather small. The peak strength is followed by a significant drop in strength; thereafter, the cracks grow significantly in width and number. Observations during post-earthquake surveys and experimental tests have shown that two types of crack patterns can be distinguished in masonry spandrels, i.e., a flexural crack pattern and a shear crack pattern (Beyer and Dazio 2012a). Shear cracking of masonry spandrels leads to a characteristic X-type crack pattern (Fig. 4b) that is similar to the shear failure of masonry piers. Flexural cracking is associated with the formation of cracks that are approximately vertical and often pass through the joints at the onset of cracking (Fig. 5a); as the cracks become wider, more and more bricks break, and the crack passes mainly through head joints and bricks (Fig. 5b).
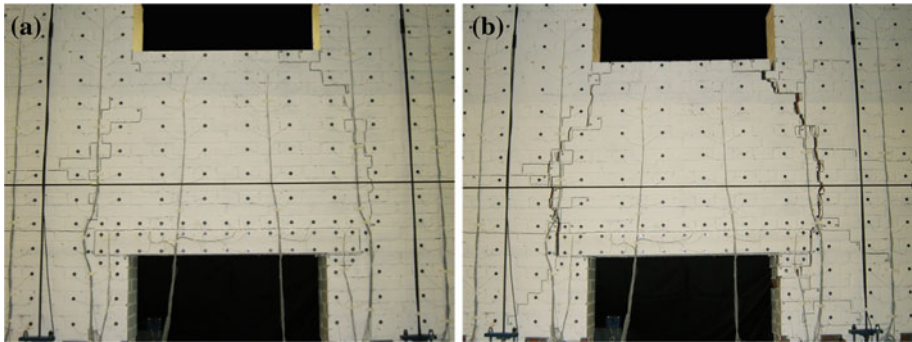
Fig. 5 Flexural cracking of spandrels: crack pattern for small rotations with flexural cracks that follow the joints **a** and crack pattern for larger rotations with flexural cracks through joints and bricks **b** (test unit TUB in Beyer and Dazio 2012a)

Shear cracking is common for squat spandrels with large axial loads, whereas flexural cracking is typical for slender spandrels or spandrels with small axial loads (Beyer and Dazio 2012a). In addition to flexural and shear types of failures, mixed failure modes have been observed, where, for example, flexural cracks develop initially but, due to the increase in axial force with increasing deformation, the residual strength after passing the peak resistance is controlled by shear failure. Sliding is not a mechanism that is capable of initiating the cracking of the spandrel because the shear force acts perpendicular to the bed joints. The sliding mechanism can, however, control the residual strength of the spandrel once flexural cracking leads to an approximately vertical rupture plane. However, in most cases the rupture plane is curved (Fig. 5b), and hence the sliding failure of spandrels is unlikely.

3 Strength models for masonry spandrels in codes

Most structural codes, such as Eurocodes 6 (CEN 2004) and 8 (CEN 2004, 2005a,b), and the Canadian standard for the design of masonry structures (CSA 2004), do not address the strength capacity of masonry spandrels. The draft version of the New Zealand code (NZSEE 2011a) for the "Assessment and improvement of URM for earthquake resistance" suggests that the capacity of spandrels can be evaluated using the mechanical models for piers. Although Eurocode 8, Parts 1 and 3 (CEN 2004, 2005a,b), do not address the strength of masonry spandrels, they permit the consideration of spandrels in the structural analysis models provided that the spandrels are well bonded to the adjacent piers. The various codes do not address the strength capacity of spandrels because experimental data and mechanical models were scarce or even unavailable at the time the codes were prepared. As a result masonry structures are often analysed with simplified approaches, i.e., the strong spandrel—weak pier approach and the weak spandrel—strong pier approach. In the strong spandrel—weak pier approach, the spandrels are modelled as rigid elements, while in the weak spandrel—strong pier approach, the contributions of spandrels are fully neglected (Cattari and Lagomarsino 2008). The FEMA 306 guidelines (FEMA 306 ATC 1998) and the Italian code OPCM 3431 (OCPM 2005) are, to our knowledge, the only standards that propose equations for the strength of masonry spandrels, and these are reviewed below.

3.1 FEMA 306

3.1.1 Spandrel strength equations in FEMA 306

At the time FEMA 306 was written, a methodology for estimating the strength of masonry spandrels did not exist (FEMA 306 ATC 1998). The authors of FEMA 306 therefore recommended that the proposed equations should only be regarded as placeholders until such research has been carried out. More than ten years after the publication of FEMA 306, the situation has hardly changed. From today's point of view, the spandrel strength models included in FEMA 306 are still unique because they allow both the peak and the residual strengths of masonry spandrels to be addressed. Note that in FEMA 306, the peak and residual strengths are referred to as the strengths of uncracked and cracked spandrels, respectively. This section summarises the strength equations in FEMA 306 and discusses their merits and faults.

Peak flexural strength: The flexural capacity of the uncracked spandrel is derived from the shear stresses in joints between bricks that are pulled out due to the opening of a flexural crack at the interface between the pier and the spandrel (FEMA 306 ATC 1998). FEMA 306 assumes that the peak shear strength τ of the mortar joints can be described by a Mohr-Coulomb relationship:

$$\tau = c + \mu\sigma \tag{1}$$

where c is the cohesion, μ is the friction coefficient and σ is the normal compressive stress acting on the joint. FEMA 306 does not introduce μ as a variable but assumes $\mu = 1.0$. Hence, FEMA 306 estimates the equivalent tensile strength due to friction in the bed joints as:

$$f_{p,bj} = 0.5 \left(0.75c + \gamma_{sp}\sigma_{pier}\right) \tag{2}$$

where $\gamma_{sp}\sigma_{pier}$ is the axial compressive stress on the bed joints at the end of the spandrel, which is expressed as a ratio of σ_{pier}, i.e., the vertical compressive stress in the adjacent pier. A ratio of 0.5 is suggested for γ_{sp}.

As a second mechanism that contributes to the equivalent tensile strength of the spandrel, FEMA 306 introduces the strength $f_{p,sj}$, which is generated by the cohesion on the side faces of the bricks if the wall consists of several wythes:

$$f_{p,sj} = 0.5 \left(0.75c\right) \tag{3}$$

The reduction factor of 0.75 on the cohesive strength c (Eqs. 2 and 3) accounts for shear transferred by the collar joints; this is because the cohesive strength is determined from in-situ tests (NZSEE 2011b). As the shear strength is determined from triplet tests (see Sect. 2.1), it can be omitted. The factor of 0.5 is assumed to be a partial safety factor and is therefore also omitted when comparing experimental and predicted strength values (see Sect. 5). Assuming a linear stress profile over the height of the spandrel and neglecting the effect of the axial force P_{sp} in the spandrel, FEMA 306 computes the peak moment resistance of the masonry spandrel as:

$$M_{p,fl} = \frac{2}{3}h_{sp} \cdot \left(f_{p,bj} \cdot t_b \cdot \frac{l_b}{2} + f_{p,sj} \cdot \frac{l_b}{2} \cdot h_b \cdot (NB - 1)\right) \cdot \frac{h_{sp}}{4\left(h_j + h_b\right)} \tag{4}$$

where NB is the number of wythes and t_b the width of one brick, i.e., the width of one wythe. The parameters h_{sp}, l_b, h_b and h_j define the height of the masonry spandrel, the length of the brick, the height of the brick and the thickness of the joint, respectively (Fig. 6). The axial force, P_{sp}, is positive when the spandrel is in compression. In our opinion, it is unclear why,
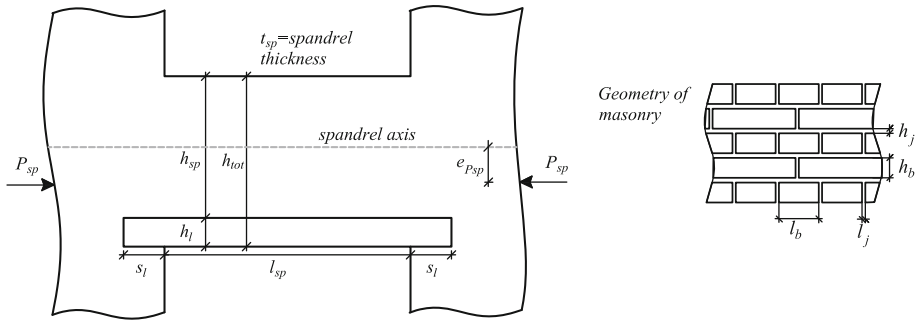
Fig. 6 General geometry of spandrel and masonry

in Eq. (4), the equivalent tensile strength is multiplied by the width of a single brick t_b and not by the width of the spandrel t_{sp}.

Peak shear strength: In FEMA 306, the peak shear strength of the spandrel is based on the model by Turnšek and Čačovič (1970):

$$V_{p,s} = f_{dt} \cdot h_{sp} \cdot t_{sp} \cdot \beta \cdot \sqrt{1 + \frac{p_{sp}}{f_{dt}}} \tag{5}$$

where f_{dt} is the diagonal tensile strength of the masonry, t_{sp} is the width of the spandrel and p_{sp} is the mean axial compressive stress in the spandrel ($p_{sp} = P_{sp}/h_{sp}t_{sp}$). The parameter β is a geometric parameter that accounts for the effect of the slenderness ratio on the shear strength. In its original version, the equation addresses the shear strength of piers, and the factor β is defined as a function of the inverse of the slenderness ratio, i.e., $0.67 \leq \beta = l_{pier}/h_{pier} \leq 1.00$ (Turnšek and Čačovič 1970; Magenes and Calvi 1997). In FEMA 306, the factor β for spandrels is defined as being equal to the slenderness ratio l_{sp}/h_{sp} of the spandrel ($0.67 \leq \beta = l_{sp}/h_{sp} \leq 1.00$). We believe, however, that this represents a typographic error and that for spandrels, the factor β should be defined in analogy to the piers as $0.67 \leq h_{sp}/l_{sp} \leq 1.00$.

Residual strength after flexural cracking: The residual flexural strength after flexural cracking is based on the same mechanism that is used in the equation for the peak flexural strength. However, it is assumed that the cohesive strength of the joints has been lost. Therefore, the residual strength of the bed joints equates to:

$$f_{r,bj} = 0.5\gamma_{sp}\sigma_{pier} \tag{6}$$

where 0.5 is a safety factor. The moment is computed by assuming a symmetric stress distribution with a rectangular shape (Fig. 7):

$$M_{r,fl} = \frac{1}{2}h_{sp} \cdot f_{r,bj} \cdot t_b \left(\frac{l_b}{2} - \Delta_s\right) \cdot \frac{h_{sp}}{2\left(h_j + h_b\right)} \tag{7}$$

The effective length, $l_b/2$, over which the brick slips is reduced by the average head joint opening Δ_s.

Residual strength after shear cracking: The residual flexural and shear strength is estimated using the same equations as those for the uncracked spandrel, but the height h_{sp} of the spandrel should be reduced to only the amount of the remaining uncracked masonry.
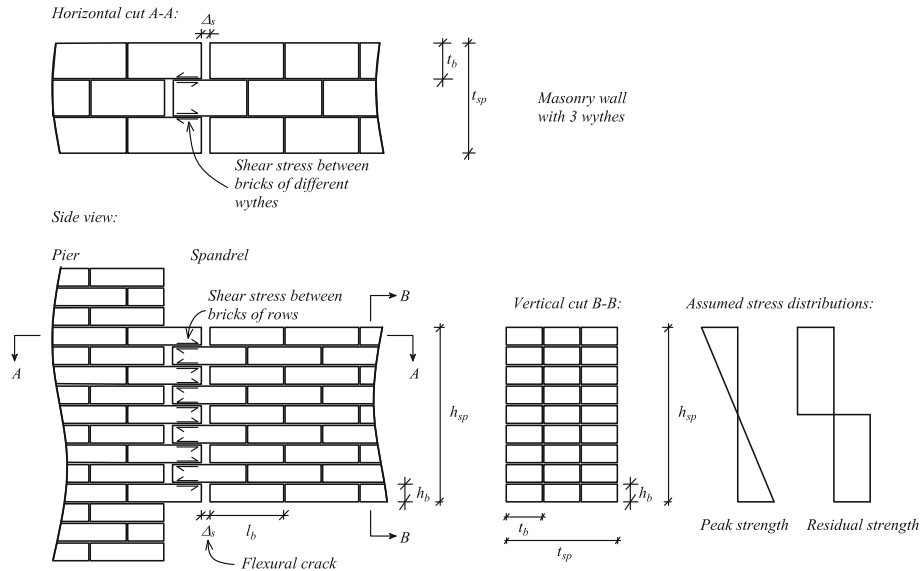
Fig. 7 Geometry and assumptions for FEMA 306 (adapted from ATC 1998)

3.1.2 Discussion of spandrel strength equations in FEMA 306

Considering the absence of experimental tests on masonry spandrels at the time of publication, the spandrel strength equations in FEMA 306 are remarkably refined. FEMA 306 does not only distinguish peak and residual strengths but also differentiates between the residual strength based on whether flexural or shear cracking has occurred. Moreover, it also considers walls with several wythes. In spite of these considerable achievements, a number of assumptions, in particular those related to the residual strength equations, seem disputable:

- FEMA 306 neglects the axial force when determining both the flexural peak and residual strengths. Experimental results (e.g., Beyer and Dazio 2012a) and numerical analyses (e.g., Cattari and Lagomarsino 2008; Milani et al. 2009) of masonry spandrels have, however, shown that the residual flexural strength, in particular, is strongly dependent on the axial force in the spandrel.
- The assumed mechanism of a flexural crack that is open over the entire height of the spandrel is not quite correct and disagrees with the assumed stress distributions (Fig. 7). For the computation of the residual flexural strength, the effective length, along which the interlocking forces are transferred, is reduced by the average head joint opening Δ_s. This seems to be an unnecessary refinement that suggests an accuracy that such models can hardly achieve. For example, for a standard brick with $l_b = 120$ mm and an average head joint opening of the flexural crack of $\Delta_s = 5$ mm, the difference in predicted strength is only 8 %.
- The stress distribution assumed for the flexural strength after flexural cracking is disputable (Fig. 7). FEMA 306 assumes a rectangular stress distribution with the compressive stress equal to the equivalent tensile stress. This is incorrect because the horizontal compressive stress can be a multiple of the equivalent tensile stress.
- The instructions for estimating the residual strength after shear cracking are unsatisfactory because recommendations for the choice of the residual height value are missing.
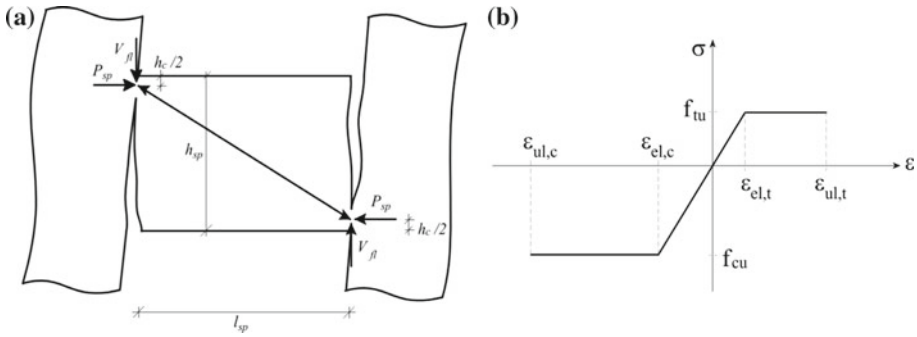
Fig. 8 Diagonal compression strut model in OPCM 3431 used to estimate the flexural capacity **a**. Stress-strain relationship for masonry by Cattari and Lagomarsino (**b**, adopted from Cattari 2007)

Moreover, for a diagonal crack through the spandrel, the effective height values vary along the length of the spandrel from the full height to zero height. It might therefore be concluded that the flexural and shear strengths after shear cracking are zero.

3.2 OPCM 3431

3.2.1 Spandrel strength equations in OPCM 3431

The Italian seismic design code OPCM 3431 (OPCM 2005) provides guidelines for computing the shear and flexural capacities of spandrel elements in URM buildings. It distinguishes between spandrel elements for which the axial forces are known and unknown. If the axial force in the spandrels is known, the spandrels are treated like piers. If it is unknown, the capacity of the spandrel can only be considered if a strut-and-tie mechanism can develop, i.e., a tension member must be present. If the axial force P_{sp} is known, the shear strength associated with the flexural mechanism of the spandrel can be computed as (Fig. 8a):

$$V_{fl} = P_{sp} \cdot \frac{h_{sp}}{l_{sp}} \left(1 - \frac{P_{sp}}{0.85 f_{hd} h_{sp} t_{sp}} \right) \qquad (8)$$

where f_{hd} is the design compressive strength of the masonry in the horizontal direction. If the axial force is unknown, the flexural capacity is computed by replacing P_{sp} with the minimum of H_p and $0.4 h_{sp} t_{sp} f_{hd}$, where H_p is the tensile strength of the horizontal tension elements, such as steel ties or ring beams.

Like FEMA 306, OPCM 3431 adopts the shear capacity model by Turnšek and Čačovič (Eq. 5) if the axial force is known. If it is unknown, the shear capacity is computed as:

$$V_s = h_{sp} t_{sp} c \qquad (9)$$

where c is the mean shear strength in the absence of compression, i.e., the mean cohesive strength. If the axial force is known, OPCM 3431 also proposes an alternative model, which computes the shear resistance as the sliding shear resistance in the compression zone:

$$V_s = h_c t_{sp} \cdot c + \mu \cdot P_{sp} \qquad (10)$$

where h_c is the depth of the compression zone in the spandrel. OPCM 3431 recommends a value of 0.4 for the friction coefficient μ.

3.2.2 Discussion of spandrel strength equations in OPCM 3431

Unlike FEMA 306, OPCM 3431 explicitly accounts for the contribution of the axial force to the flexural strength; this represents a considerable improvement. However, some assumptions underlying the spandrel strength equations in OPCM 3431 can be discussed:

- OPCM 3431 does not explicitly state whether it addresses the peak or residual strength values. The equation for the flexural strength model addresses the residual strength after flexural cracking (model with a diagonal compression strut and stress block). On the contrary, the shear strength models seem to address the peak strength before severe shear cracking because the models rely on the diagonal tensile strength and cohesion, respectively.
- Equation (10) was developed for the sliding failure of walls. However, in spandrels, interlocking bricks tend to prevent sliding failure at peak strength. At residual strength, the failure plane created by the flexural crack is often not perfectly planar; for this reason, as outlined in Sect. 2.1.1, sliding failure is considered to be a rare failure mode for spandrels.
- If the axial force in the spandrel is unknown, estimating the spandrel capacity based on the axial force $P_{sp} = \min(H_p, 0.4h_{sp}t_{sp}f_{hd})$ overestimates the maximum spandrel shear force because, in general, the maximum axial force P_{sp} in the spandrel will be less than the limit values of H_p and $0.4h_{sp}t_{sp}f_{hd}$ (Betti et al. 2008). Hence, the axial force in the spandrel needs to be estimated from a numerical or mechanical model that captures the axial, flexural and shear flexibilities of the piers, spandrels and, if present, tension elements such as steel ties.

4 Strength models for masonry spandrels in the literature

Most equivalent frame analysis studies of URM buildings utilise some or all of the spandrel strength equations in OPCM 3431 (see Table 2). However, additional equations for estimating the spandrel strength have been proposed by different research groups, i.e., Magenes and Della Fontana (1998), Cattari and Lagomarsino (2008), and Betti et al. (2008). The section considers only those models that present closed-form expressions for the strength of masonry spandrels. Approaches that are based on numerical models of spandrels (e.g., Milani et al. 2009; Sabatino and Rizzano 2011) are not included in this summary. The following two sections summarise the proposed equations for estimating the shear and flexural strengths of masonry spandrels.

4.1 Shear strength of masonry spandrels

Magenes and Della Fontana (1998) were the first to study the effect of spandrels on the behaviour of masonry buildings and therefore influenced the development of the treatment of masonry spandrels in the Italian code OPCM 3431. In their analyses, they estimated the spandrel strength in a manner similar to Eq. (9):

$$V_s = h_{sp}t_{sp}c_{red} \tag{11}$$

where h_{sp} and t_{sp} are the height and width of the masonry spandrel, respectively (Fig. 6) and c_{red} is the reduced cohesion of the mortar bed joints (Mann and Müller 1982):

$$c_{red} = c \frac{1}{1 + 2\left(h_b + h_j\right)/\left(l_b + l_j\right)} \tag{12}$$

Table 2 Overview of models implemented in equivalent frame analysis studies on URM buildings for computing spandrel strengths

Studies with equivalent frame analyses of URM buildings	Implemented mechanical models for computing the spandrel strengths				Mechanical models A–D
	A	B	C	D	
Magenes and Della Fontana (1998)		×			Shear strength model by Turnšek and Čačovič (1970) for diagonal tension:
Magenes (2000)		×		×[a]	$V_{p,s} = f_{dt} \cdot h_{sp} \cdot t_{sp} \cdot \beta \cdot \sqrt{1 + \frac{p_{sp}}{f_{dt}}}$ (A)
Salonikios et al. (2003)	×			×[b]	Sliding shear resistance:
Lagomarsino et al. (2006)	×	×	×	×[a]	$V_s = h_{sp} t_{sp} c$ (B)
Pasticier et al. (2008)		×		×[a]	Sliding shear resistance as a function of compression zone:
Chen et al. (2008)	×		[c]		$V_s = h_c t_{sp} \cdot c + \mu \cdot P_{sp}$ (C)
Mallardo et al. (2008)	×		×	×[a]	Flexural resistance:
Belmouden and Lestuzzi (2009)	×		×	×[a]	$V_{fl} = P_{sp} \cdot \frac{h_{sp}}{l_{sp}} \left(1 - \frac{P_{sp}}{\alpha f_{hd} h_{sp} t_{sp}}\right)$ (D)
Amadio et al. (2011)		×		×[a]	
Sabatino and Rizzano (2011)		×	[c]		

[a] $\alpha = 0.85$, [b] $\alpha = 0.70$, [c] The flexural resistance was computed by means of a section analysis that included an equivalent tensile strength due to the interlocking of the bricks

where h_b, h_j, l_b and l_j are the dimensions of the bricks and joints, respectively (Fig. 6). To our knowledge, additional models for estimating the shear strength of masonry spandrels have not been published, but previous research concentrated on developing flexural strength models of spandrels, which are discussed in the following section.

4.2 Flexural strength of masonry spandrels

All the proposed flexural strength models for masonry spandrels are based on the assumption of a linear strain profile over the section. The proposed models can be grouped into two groups, i.e., models that consider the equivalent tensile strength of the masonry due to the interlocking of bricks and models that neglect it. The mechanism of the equivalent tensile strength due to the interlocking of bricks was previously described by FEMA 306 (see Sect. 3.1.1).

4.2.1 Flexural strength models considering the equivalent masonry tensile strength

Cattari and Lagomarsino (2008) applied the approach of an equivalent tensile strength for computing the flexural resistance of a masonry spandrel but neglected the cohesive strength of the mortar joints. They refined the equivalent tensile strength by introducing an additional tension limit that accounts for the limited tensile strength f_{bt} of the bricks. Hence, their model also accounts for the possibility of a flexural crack through the head joints and bricks. The equivalent tensile strength is computed as:

$$f_{tu} = \min\left(\mu \gamma_{sp} \sigma_{pier} \frac{l_b}{2(h_j + h_b)}; \frac{f_{bt}}{2}\right)$$ (13)

Cattari and Lagomarsino proposed a value of 0.65 for γ_{sp}, which is slightly higher than the value proposed by FEMA 306 ($\gamma_{sp} = 0.5$). Based on the stress-strain relationship shown in Fig. 8b, the flexural capacity of the masonry spandrel is evaluated for an axial force P_{sp}. The complete set of equations is provided in Cattari (2007). In particular for low values of P_{sp}, the model yields larger flexural capacities than Eq. (8), which neglects the tensile stresses due to the interlocking of the bricks (Cattari and Lagomarsino 2008).

Adding the tensile failure of the bricks as an additional failure mode describes the failure domain more accurately. However, in the present form, the tensile failure of the bricks is only the controlling failure criterion if the compressive stress in the piers is large, i.e., when the clamping stresses $\gamma_{sp}\sigma_{pier}$ on the bed joints at the interface of the spandrel and the pier are rather large. This is contradictory to observations from tests, which have shown that at the residual state the flexural cracks often pass through the bricks (Fig. 5b). However, we believe that the bricks often break due to a combination of tensile force, local bending and stress concentrations rather than a tensile force alone.

4.2.2 Flexural strength models neglecting the equivalent masonry tensile strength

Betti et al. (2008) proposed, as an alternative to Eq. (8), two additional equations for estimating the ultimate flexural capacity of a spandrel. For large axial compressive forces P_{sp}, they proposed:

$$M_u = \frac{h_{sp}^2 t_{sp}}{6} \left(0.85 f_{hm} - p_{sp} \right) \tag{14}$$

For small axial compressive forces or tensile forces ($P_{sp} < 0$), they proposed:

$$M_u = \frac{h_{sp}^2 t_{sp}}{6} \left(f_{tm} + p_{sp} \right) \tag{15}$$

where f_{tm} is the tensile strength of the masonry, i.e., the tensile strength of the mortar joints. The formulae are based on the assumption of a linear stress distribution. This suggests that the authors intended to address the peak flexural resistance rather than the residual flexural resistance. Unlike Eqs. (4) and (13), they do not, however, consider the equivalent tensile strength due to the interlocking mechanism. For most masonry spandrels, the axial compressive stress p_{sp} in the spandrel is rather low; Eq. (14) should, therefore, rarely be relevant.

Parisi and Augenti (2011) compared the flexural strength domain of masonry spandrels obtained from section analyses for different constitutive models for the masonry. The masonry was assumed to act only in compression. Their results showed that the flexural strength is relatively insensitive to the assumed constitutive models for axial load ratios $P_{sp}/h_{sp}t_{sp}f_{hd}$ less than ~0.2, which should apply to most spandrels. For such axial load ratios, their models yield similar results to the flexural strength equation in OPCM 3431 (Eq. 8). If the axial force ratio is greater than ~0.3, the assumed constitutive model can have a significant influence on the estimated flexural capacity of the spandrel. For conservative estimates, they recommended their own constitutive model, or an elasto-perfectly brittle constitutive relationship, to describe the behaviour of masonry in compression.

5 Comparison of predicted strength values with experimental results

This section compares the proposed equations for estimating the spandrel strength to the experimental results obtained from the four spandrel tests presented in Sect. 2. The section is

divided into three parts, which summarise the applied equations, compare the predicted and experimental strength values and discuss the findings, respectively.

5.1 Summary of equations for predicting spandrel strength

The comparison is based on the equations included in the OPCM 3431 and FEMA 306 codes and the flexural strength models proposed by Cattari and Lagomarsino (2008) and by Betti et al. (2008). The other equations summarised in Sect. 4 are not included for the following reasons: (i) Magenes and Della Fontana (1998) approach for computing the shear strength of spandrels is now included in the Italian code OPCM 3431. (ii) As outlined in Sect. 4.2.1, the constitutive model proposed by Parisi and Augenti (2011) is only relevant for axial load ratios greater than approximately 0.2–0.3. The axial load ratios of the four spandrels varied between zero and 0.04 and are therefore much less than that is relevant for their model.

The spandrel strength equations included in the comparison are summarised in Table 3. As suggested in OPCM 3431, if the spandrel strength is originally given in terms of the bending moment, an equivalent shear strength is computed by assuming that the spandrel is subjected to double bending. The material properties are summarised in Table 1. The diagonal tensile strength of the masonry f_{dt} was not determined experimentally. To include the equation in the comparison, a value of $f_{dt} = 0.15$ MPa was assumed for all spandrels (e.g. Turnšek and Čačovič 1970). The horizontal strength f_{hd} of the masonry was also not determined experimentally. As a first approximation, f_{hd} is assumed as equal to the vertical compressive strength of the masonry f_{cm} (Beyer and Dazio 2012a). The tensile strength of the masonry joints, which is required for the model by Betti et al. (2008), was estimated from the experimentally determined values for cohesion and friction using the parabolic tension cut-off criterion for mortar joints proposed by Rots and Lourenço (1993):

$$f_{hj} = \frac{c}{2\mu} \tag{16}$$

The mean height of a brick and a joint together was 74 mm. The length of a brick and the width of a head joint were assumed to be 120 mm and 10 mm, respectively. The reduced cohesion according to Mann and Müller (1982), which was used to compute the shear strength according to OPCM 3431, therefore equates to $c_{red} = 0.47c$.

Cattari's and Lagomarsino's flexural strength model, which was developed for beam elements with concentrated plasticity at their ends, is based on an elasto-plastic stress-strain relationship. Hence, its rigorous application requires the assumption of a strain profile that is related to the global spandrel deformation. For comparison with the experimental results, the elasto-plastic stress-strain relationship was replaced by a rigid-plastic relationship, and it was further assumed that the tensile and compressive strain capacity was unlimited. The strength was therefore independent of the curvature. Note that the tensile strength of the bricks used for the construction of the test units was rather large (see Table 1). For this reason, the equivalent tensile strength was controlled by the limited strength of the interlocking mechanism and not by the tensile failure of the bricks.

The objective is to compute the strength values without applying any safety factors. For this reason, all factors in the FEMA equations that were interpreted as safety factors or factors that account for particularities of the in-situ test methods (see Sect. 3.1.1) were set to unity. Note also that in the FEMA equation describing the residual flexural strength, the brick width was replaced by the spandrel width (see Sect. 3.1.1).

Table 3 Summary of equations for predicting the spandrel strength

OPCM 3431 (2005)	Flexure	$V_{fl} = P_{sp} \cdot \frac{h_{sp}}{l_{sp}} \left(1 - \frac{P_{sp}}{0.85 f_{hd} h_{sp} t_{sp}}\right)$	Eq. (8)[a]
	Shear 1	$V_s = h_{sp} t_{sp} c_{red}$ with $c_{red} = c \frac{1}{1+2(h_j+h_b)/(l_b+l_j)}$	Eqs. (11) & (12)
	Shear 2	$V_s = h_c t_{sp} \cdot c_{red} + 0.4 \cdot P_{sp}$ with $h_c = \frac{P_{sp}}{0.85 f_{hd} t_{sp}}$	Eq. (10)
		and c_{red} as in Shear 1	
FEMA 306 ATC (1998)	Flexure, peak	$V_{p,fl} = \frac{2}{l_{sp}} \cdot \frac{2}{3} h_{sp} \cdot f_{p,tot} \cdot \frac{h_{sp}}{4(h_j+h_b)}$	Eq. (4)[a]
		with $f_{p,tot} = f_{p,bj} \cdot t_b \cdot \frac{l_b}{2} + f_{p,sj} \cdot \frac{l_b}{2} \cdot h_b \cdot (NB-1)$ and $f_{p,bj} = c + 0.5 \cdot \sigma_{pier}$, NB = 1	
	Flexure, residual	$V_{r,fl} = \frac{2}{l_{sp}} \cdot \frac{1}{2} h_{sp} \cdot f_{r,bj} \cdot t_{sp} \left(\frac{l_b}{2} - \Delta_s\right) \cdot \frac{h_{sp}}{2(h_j+h_b)}$ with $f_{r,bj} = 0.5\sigma_{pier}$ and $\Delta_s = 0$	Eq. (7)[a]
Turnšek and Čačovič (1970)	Shear	$V_{p,s} = f_{dt} \cdot h_{sp} \cdot t_{sp} \cdot \beta \cdot \sqrt{1 + \frac{P_{sp}}{f_{dt}}}$ with $0.67 \leq \frac{h_{sp}}{l_{sp}} \leq 1.00$	Eq. (5)
Cattari and Lagomarsino (2008)	Flexure	$V_{fl} = \frac{2}{l_{sp}} \cdot t_{sp} \cdot \left(0.85 f_{hd} h_c \left(\frac{h_{sp}}{2} - \frac{h_c}{2}\right) + f_{tu} (h_{sp} - h_c) \frac{h_c}{2}\right)$ with $f_{tu} = \min\left(\mu \cdot 0.65 \cdot \sigma_{pier} \frac{l_b}{2(h_j+h_b)}; \frac{f_{bt}}{2}\right)$, $h_c = \frac{p_{sp}+f_{tu}}{0.85 f_{hd}+f_{tu}} h_{sp}$	Eq. (13)
Betti et al. (2008)	Flexure	$V_{fl} = \frac{2}{l_{sp}} \cdot \frac{h_{sp}^2 t_{sp}}{6} (f_{tm} + p_{sp})$ with $f_{tm} = \frac{c}{2\mu}$	Eqs. (15) & (16)[a]

[a] End moments are converted to a shear force assuming the spandrel is subjected to double bending

5.2 Comparison of predicted and experimental strength values

The comparisons of the predicted values with the experimentally determined strength values are shown in Figs. 9, 10, 11 and 12. In the test results, only the positive and negative envelopes of the cyclic force-deformation curves are plotted. The plots include both the shear forces and the axial forces of the spandrels. The forces are plotted against the average pier rotation. TUA developed a mixed flexural-shear mechanism, TUB developed a flexural mechanism and TUC developed a shear mechanism. TUD developed flexural cracks at the beginning of the test. Due to the strong axial restraint, which caused a significant increase in the axial force with increasing deformation, the mechanism changed rapidly to a mechanism dominated by shear cracks (a more detailed description of the failure mechanisms is contained in Beyer and Dazio (2012a)). Hereafter we focus on the comparison between the predicted and observed strength values for TUB and TUC, which developed a clear flexural and a clear shear mechanism, respectively.

The results for TUB are shown in Fig. 10. All predicted values, which estimate the flexural strength, are plotted in red, while those predicting the shear strength are plotted in blue. The model by Betti et al. (2008), which is supposedly intended to estimate the peak strength, yields by chance very similar values as the FEMA equation for the residual flexural strength. It underestimates the peak strength by approximately 70 % and therefore seems to be unsuitable for estimating the peak flexural strength of the spandrel. This indicates that for the peak strength, the equivalent tensile strength due to interlocking should be considered. Indeed,
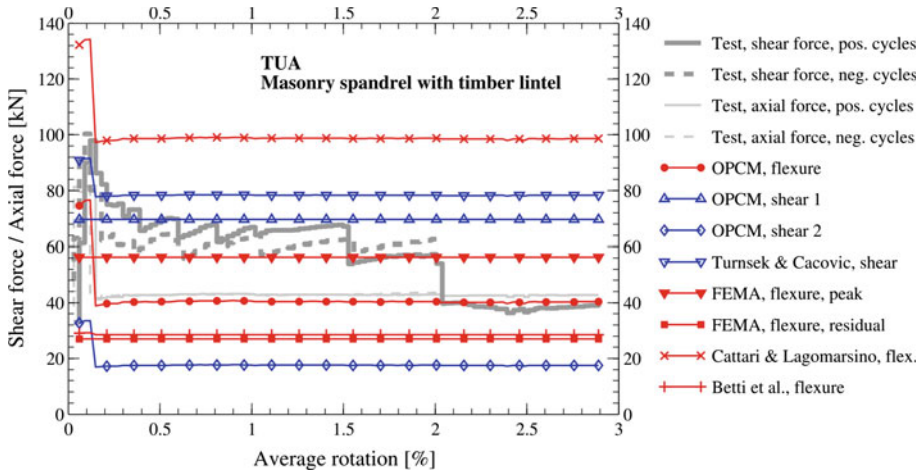
Fig. 9 TUA: comparison of predicted and experimentally determined strength values
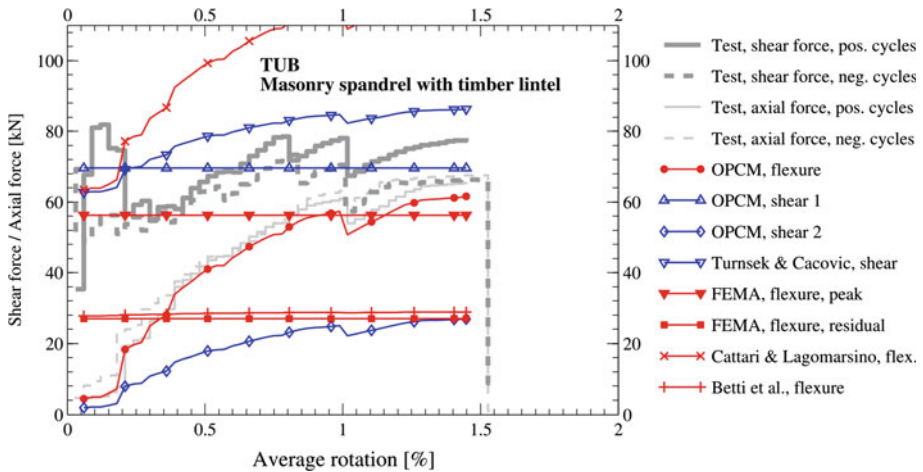

Fig. 10 TUB: comparison of predicted and experimentally determined strength values

the model proposed by Cattari and Lagomarsino and the FEMA equation for the flexural peak strength, which both account for the equivalent tensile strength due to interlocking, underestimate the peak strength only by approximately 20–30 %. The OPCM equation for flexural strength underestimates the experimentally determined residual flexural strength of the spandrel once the spandrel has cracked by approximately 20 kN, which corresponds to approximately 25–35 % of the actual strength. The FEMA equation for the residual strength, however, grossly underestimates the strength of the spandrel after cracking. This can be attributed to the fact that FEMA does not account for the axial force in the spandrel when computing its flexural strength. To summarise, the model by Cattari and Lagomarsino and the FEMA equation for the flexural peak strength seem to be best suited for estimating the peak flexural strength, while the OPCM equation for flexural strength best captures the strength after cracking. However, all three equations underestimate the actual strength values by approximately 25 %.
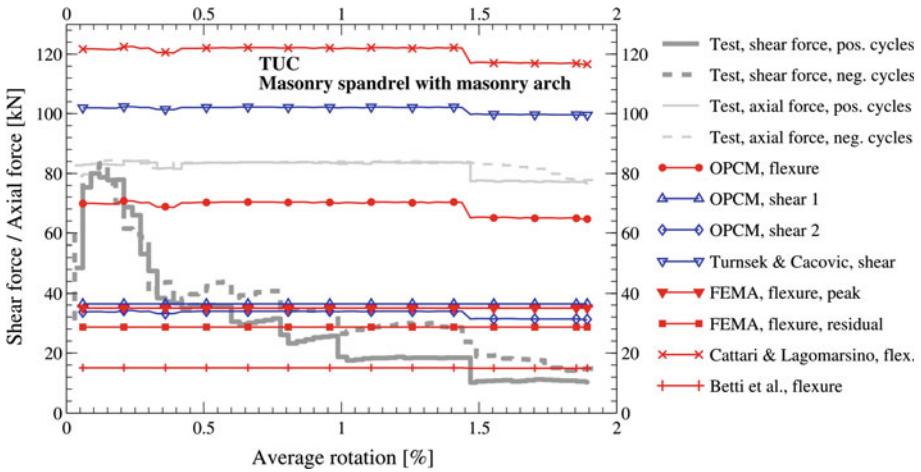
Fig. 11 TUC: comparison of predicted and experimentally determined strength values
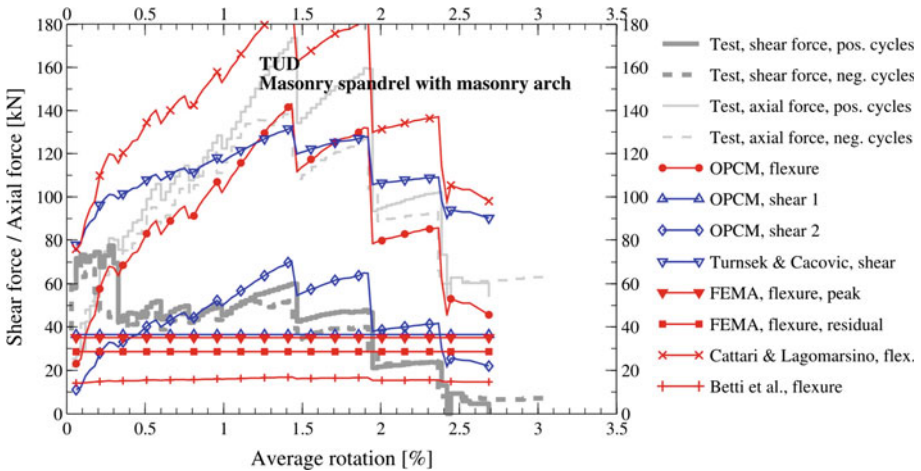

Fig. 12 TUD: comparison of predicted and experimentally determined strength values

Figure 10 shows the results for TUC, which developed a shear failure mechanism. The two OPCM equations for the shear strength lead to similar values, which are very close to the experimentally determined residual strength. It is surprising that the first OPCM shear equation, which is based on the cohesive strength of the spandrel alone, matches the residual shear strength of the spandrel so well, as the cohesive strength of the joints is lost after the joints undergo some sliding movement associated with the shear mechanism. The shear strength equation by Turnšek and Čačovič overestimates the actual peak strength by approximately 30 %. The reader is reminded, however, that the diagonal tensile strength, which enters into this equation, was not obtained from material tests but was merely roughly estimated as $f_{dt} = 0.15$ MPa. For a diagonal tensile strength of $f_{dt} = 0.10$ MPa, the predicted strength would match the experimentally obtained peak strength. Note also that the set of FEMA equations suggests that a flexural mechanism would form rather than a shear mechanism. As outlined above, the FEMA equations for the flexural strength do not account for the axial

force of the spandrel and therefore underestimate the flexural capacity. This leads to incorrect conclusions regarding the dominant failure mechanism, in particular, for spandrels with relatively large axial forces, such as TUC. The equation by Cattari and Lagomarsino therefore seems to be the better choice when estimating the peak flexural strength of a spandrel.

5.3 Summary of findings from the comparison of predicted and experimental strength values

The results for TUA and TUD, which developed mixed failure mechanisms, show very similar trends as those for TUB and TUC, which developed a flexural and a shear mechanism, respectively. Grouped according to failure mode and peak or residual strength, the following observations can be summarised:

Peak flexural strength: Cattari's and Lagomarsino's model gave the best estimate for the peak flexural strength capacity of the spandrels. To apply the model to TUA-TUD, the elasto-plastic stress-strain relationship with a limited strain capacity was replaced by a rigid-plastic relationship with an unlimited strain capacity. This modification might account for the fact that the model sometimes overestimates the peak strength, although it neglects the cohesive strength of the bed joints and the tensile strength of the head joints. FEMA 306, which is also based on an interlocking mechanism but assumes a linear stress distribution (Fig. 7), neglects the effect of the axial force in the spandrel and therefore tends to underestimate the peak flexural strength. The equation by Betti et al. (2008) neglects the equivalent tensile strength due to the interlocking mechanism and only considers the tensile strength of the mortar in the head joints. As a result, the flexural peak strength of the spandrels is considerably underestimated.

Residual strength after flexural cracking: The model proposed by OPCM 3431, which is based on a diagonal compression strut, seems to be the most suitable approach for estimating the residual strength after flexural cracking, although it tends to underestimate the experimentally obtained strength to some extent. Observations from the experimental tests indicate that the difference in strength can possibly be attributed to the contribution of timber lintels or masonry arches to the spandrel strength. The equation in FEMA 306, which is based on the interlocking mechanism of the bricks, underestimates the actual residual strength significantly because it neglects, as for the peak strength, the effect of the axial force. Moreover, it was observed that at the residual state, cracks pass through many bricks, and the interlocking failure mechanism is therefore impaired. This observation suggests that the residual flexural strength should not be based on the interlocking failure mechanism, which should be confirmed through further tests.

Peak shear strength: For the peak shear strength of masonry spandrels, FEMA 306 and OPCM 3431 propose the model by Turnšek and Čačovič (1970). Because the diagonal tensile strength of the masonry was not determined from material tests, a rather rough estimate was necessary to apply the model to the spandrels. The comparison suggests, however, that the model by Turnšek and Čačovič (1970) is able to estimate the peak shear strength of the spandrel.

Residual strength after shear cracking: The two shear strength models in OPCM 3431 are not explicitly referred to as models for estimating the residual spandrel strength after shear cracking. Indeed, the fact that shear strength is, in both cases, a function of the cohesion could suggest that they are aimed at estimating the peak shear strength. The first OPCM shear equation neglects the influence of the axial force P_{sp} on the shear strength of the spandrel, although experimental observations have suggested that at the residual state, the axial

load plays a particularly important role. However, the comparison to the experimental results showed that, in particular, the first OPCM shear equation yields good estimates of the residual shear strength for the four analysed spandrels. Because this finding seems somewhat contrary to the mechanical understanding, we recommend that the validity of this conclusion should be carefully revisited once more experimental results become available. The second OPCM shear equation computes the shear strength as the sliding resistance of the compression zone. It yields a good estimate of the shear strength of TUC but underestimates the shear strength of TUA. As outlined above, we do not consider sliding failure to be a particularly critical failure mode for estimating either the peak strength or the residual strength of masonry spandrels.

6 Conclusions

Despite the lack of experimental data for masonry spandrels, a number of strength models for spandrels have been proposed in the past, both in codes and in scientific papers. The objective of this paper was to give an overview of the existing strength models, apply these models to spandrels that have been recently tested experimentally and, based on the comparison, formulate recommendations for future strength models for spandrels. The experimentally determined force-deformation relationships of spandrels show two different strength levels: a peak strength, which is attained for rather small deformation demands, and a residual strength, which is typically much lower than the peak strength but which is associated with a much larger deformation capacity than the peak strength. For this reason, new strength models should continue the path set by FEMA 306 and clearly distinguish between peak and residual strength values. Based on the comparison of mechanical models and experimental results, a number of models were identified that seem particularly well suited for estimating the peak and residual strength of a masonry spandrel when it develops either a flexural or shear failure mechanism.

All the models address only the behaviour of plane masonry spandrels. However, most spandrel elements contain a timber lintel or a masonry arch next to the masonry spandrel. None of the reviewed models accounts for the contribution of the lintel or the arch to the strength of the spandrel element or discusses the interaction of the lintel or the arch with the masonry spandrel. The crack pattern and mechanisms that developed during the testing of the four spandrels (Beyer and Dazio 2012a) suggested that these elements might play an important role, in particular, after cracking, i.e., for the residual strength. Future work should therefore investigate the influence of lintels and arches on the behaviour of the spandrel and develop models that account for the contribution of a lintel or a masonry arch to the strength of the spandrel.

The axial force in the spandrel greatly influences whether a flexural or a shear mechanism develops (Beyer and Dazio 2012a). The comparison of predicted and experimentally obtained values also showed that, with the exception of the first shear model in OPCM 3431 (Eq. 9), only models that account for the axial force in the spandrel yield good estimates of the observed spandrel strengths. The axial force should therefore be included in future strength models for spandrels. The challenge is, however, to estimate the axial force in the spandrel. The axial force in the spandrel can be caused by the restraining effect of steel ties and piers as well as the redistribution of shear forces between piers. The two estimates of axial forces in OPCM 3431 are based on the tensile failure of the tie and the compressive failure of the spandrel, respectively. However, such estimates might considerably overestimate the actual axial forces in the spandrel and, therefore, the strength of the spandrel and ultimately the seismic resistance of the building. It is therefore recommended to use numerical models

to estimate the axial force in the spandrels. Such models should ideally capture the axial, shear and flexural stiffnesses of piers and spandrels, including the reduction of the stiffness with cracking, as well as the elongation of the spandrel due to shear and flexural cracking. In particular, the latter might be difficult to include in simple equivalent frame models, and future research should therefore more closely investigate the limitations and the range of applicability of such models.

References

Amadio G, Rinaldin G, Macorini L (2011) An equivalent frame model for nonlinear analysis of reinforced masonry buildings under in-plane cyclic loading. In: Proceedings of the ANIDIS 2011 convention on seismic engineering, Sep 18–22, 2011. Bari, Italy

ATC (1998) FEMA-306 Evaluation of earthquake damaged concrete and masonry wall buildings. Basic Procedures Manual, Applied Technology Council, Washington DC

Augenti N, Parisi F, Prota A, Manfredi G (2011) In-plane lateral response of a full-scale masonry subassemblage with and without an inorganic matrix-grid strengthening system. J Comp Constr 15(4):548–590

Belmouden Y, Lestuzzi P (2009) An equivalent frame model for seismic analysis of masonry and reinforced concrete buildings. Constr Build Mater 23(1):40–53

Benedetti D, Carydis P, Pezzoli P (1998) Shaking table tests on 24 simple masonry buildings. Earthq Eng Struct Dyn 27(1):67–90

Benedetti D, Carydis P, Limongelli MP (2001) Evaluation of the seismic response of masonry buildings based on energy functions. Earthq Eng Struct Dyn 30(7):1061–1081

Braga F, Liberatore D (1990) A finite element for the analysis of the response of masonry buildings. In: Proceedings of 5th North American masonry conference, June 3–6, 1990. Urbana-Champaign, USA

Betti M, Galano L, Vignoli A (2008) Seismic response of masonry plane walls: A numerical study on spandrel strength. In: Proceedings of the 2008 seismic engineering conference commemorating the 1908 Messina and Reggio Calabria earthquake, AIP conference proceedings, July 8–11, 2008. Reggio Calabria, Italy

Beyer K and Dazio A (2012a) Quasi-static cyclic tests on masonry spandrels. Accepted for publication in Earthq Spectra (article available on http://eesd.epfl.ch/page-18604-en.html)

Beyer K and Dazio A (2012b) Quasi-static monotonic and cyclic tests on composite spandrels. Accepted for publication in Earthq Spectra (article available on http://eesd.epfl.ch/page-18604-en.html)

Calderoni B, Cordasco EA, Guerriero L, Lenz P (2008) Experimental analyses of yellow tuff spandrels of postmedieval buildings in the Naples area. In: Proceedings of the 2008 seismic engineering conference commemorating the 1908 Messina and Reggio Calabria earthquake, AIP conference proceedings, July 8–11, 2008. Reggio Calabria, Italy

Cattari S (2007) Modellazione a telaio equivalente di strutture esistenti in muratura e miste muratura-c.a.formulazione di modelli sintetici. Doctoral Thesis (in Italian), University of Genoa, Italy

Cattari S, Lagomarsino S (2008) A strength criterion for the flexural behaviour of spandrels in un-reinforced masonry walls. In: Proceedings of the 14th world conference on earthquake engineering, Oct 12–17, 2008. Beijing, China

CEN (2004) Eurocode 8 Design of structures for earthquake resistance—Part 1: General rules, seismic actions and rules for buildings, EN 1998-1:2004, European Committee for Standardisation, Brussels, Belgium

CEN (2005) Eurocode 6 Design of masonry structures—Part 1-1: General rules for reinforced and unreinforced masonry structures, EN 1996-1:2005, European Committee for Standardisation, Brussels, Belgium

CEN (2005) Eurocode 8 Design of structures for earthquake resistance—Part 3: General rules, seismic actions and rules for buildings, EN 1998-3:2005, European Committee for Standardisation, Brussels, Belgium

Chen SY, Moon FL, Yi T (2008) A macroelement for the nonlinear analysis of in-plane unreinforced masonry piers. Eng Struct 20(8):2242–2252

CSA (2004) Design of masonry structures S304.1. Canadian Standards Association, Ontario, Canada

Foraboschi P (2009) Coupling effect between masonry spandrels and piers. Mater Struct 42(3):279–300

Gambarotta L, Lagomarsino S (1997) Damage models for the seismic response of brick masonry shear walls, Part II: the continuum model and its applications. Earthq Eng Struct Dyn 26(4):441–462

Gattesco N, Clemente I, Macorini L, Noè S (2008) Experimental investigation of the behaviour of spandrels in ancient masonry buildings. In: Proceedings of the 14th world conference on earthquake engineering, Oct 12–17, 2008. Beijing, China

Graziotti F, Magenes G, Penna A (2009) Progetto di una sperimentazione su elementi di fascia muraria, Rapporto Reluis (in Italian). Allegato 4.3-UR01-1, Università di Pavia e EUCENTRE, Pavia, Italy

Haach GV, Vasconcelos G, Lourenço PB (2012) Experimental analysis of reinforced concrete block masonry spandrels using pre-fabricated planar trussed bars. Constr Build Mater 26(1):156–166

Lagomarsino S, Penna A, Galasco A (2006) TREMURI program: seismic analysis program for 3D masonry buildings. Theory and user manual. University of Genoa, Genoa

Lourenço PB (1996) Computational strategies for masonry structures. Doctoral Thesis, Technical University Delft, The Netherlands

Magenes G (2000) A method for pushover analysis in seismic assessment of masonry buildings. In: Proceedings of the 12th world conference on earthquake engineering, Jan 30–Feb 4, 2000. Auckland, New Zealand

Magenes G, Calvi GM (1997) In-plane seismic response of brick masonry walls. Earthq Eng Struct Dyn 26(11):1091–1112

Magenes G, Della Fontana A (1998) Simplified non-linear seismic analysis of masonry buildings. In: Proceedings of the British masonry society, Oct 13–15, 1998. London, UK

Magenes G, Menon A (2009) A review of the current status of seismic design and assessment of masonry buildings in Europe. J Struct Eng SERC Chennai 35(6):247–256

Magenes G, Kingsley GR, Calvi GM (1995) Seismic testing of a full-scale, two-story masonry building: Test procedure and measured experimental response. Experimental and numerical investigation on a brick masonry building prototype Rep. No. 3.0, Gruppo Nazionale La Difesa Dai Terremoti, University of Pavia, Pavia, Italy

Magenes G, Morandi P, Manzini C, Morandi O, Bolognini D (2006) SAM II—Software for the simplified analysis of masonry buildings. Theory and user manual. University of Pavia and EUCENTRE, Pavia

Mallardo V, Malvezzi R, Milani E, Milani G (2008) Seismic vulnerability of historical masonry buildings: a case study in Ferrara. Eng Struct 30(8):2223–2241

Mann W, Müller H (1982) Failure of shear-stressed masonry—An enlarged theory, tests and application to shear walls. In: Proceedings of the British ceramic society vol 30, pp 223–235

Milani G, Beyer K, Dazio A (2009) Upper bound analysis of meso-mechanical spandrel models for the push-over analysis of 2D masonry frames. Eng Struct 31(7):2696–2710

NZSEE (2011a) Assessment and improvement of unreinforced masonry buildings for earthquake resistance. Draft guideline, New Zealand Society for Earthquake Engineering, Wellington, New Zealand

NZSEE (2011b) Commentary to assessment and improvement of unreinforced masonry buildings for earthquake resistance. Draft commentary, New Zealand Society for Earthquake Engineering, Wellington, New Zealand

OPCM (2003) OPCM 3274—Primi elementi in materia di criteri generali per la classificazione sismica del territorio nazionale e di normative tecniche per le costruzioni in zona sismica, 20/03/2003 (in Italian)

OPCM (2005) OPCM 3431—Ulteriori modifiche ed integrazioni all OPCM 3274/03, 09/05/2005 (in Italian)

Parisi F, Augenti N (2011) Evolutionary strength domains of unreinforced masonry spandrel panels including strain softening. In: Proceedings of the 9th Pacific conference on earthquake engineering, April 14–16, 2011. Auckland, New Zealand

Pasticier L, Amadio C, Fragiacomo M (2008) Non-linear seismic analysis and vulnerability evaluation of a masonry building by means of the SAP2000 V.10 code. Earthq Eng Struct Dyn 37(3):467–485

Penna A (2010) Tools and strategies for the performance-based seismic assessment of masonry buildings. In: Proceedings of the international workshop on protection of built environment against earthquakes, Aug 27–28, 2010. Ljubljana, Slovenia

Rots JG and Lourenço PB (1993) Fracture simulations of masonry using non-linear interface elements. In: Proceedings of the 6th North American masonry conference, Philadelphia, USA

Sabatino R and Rizzano G (2011) A simplified approach for the seismic analysis of masonry structures. The Open Construction and Build. Technol J 5(Suppl. 1-M7):97–104

SAI (1998) Strengthening existing buildings for earthquake (AS 3826). Standards Australia International, Sydney

SAI (2001) Masonry Structures (AS 3700). Standards Australia International, Sydney

Salonikios T, Karakostas C, Lekidis V, Anthoine A (2003) Comparative inelastic pushover analysis of masonry frames. Eng Struct 25(12):1515–1523

Tomaževič M (1987) Dynamic modelling of masonry buildings: storey mechanism model as a simple alternative. Earthq Eng Struct Dyn 15(6):731–749

Turnšek V, Čačovič F (1970) Some experimental results on the strength of brick masonry walls. In: Proceedings of the 2nd international brick masonry conference, Stoke on Trent, United Kingdom, pp 149–156
Yi T, Moon FL, Leon RT, Kahn LF (2006) Lateral load tests on a two-story unreinforced masonry building. J Struct Eng ASCE 132(5):652–653